Homology Modelling, Phylogenetic Analysis, and Molecular Docking of Glutamine Aminotransferase, gatD from *Clostridium botulinum*

Praveen Kumar [1*], Archana G. Mohanan [2], Anil Kumar AK [1]

[1] *Govt. College for Women, Thiruvananthapuram, Kerala, India, 695014*

[2] *Rajiv Gandhi Centre for Biotechnology, Thiruvananthapuram, Kerala, India*

Address for Correspondence: Praveen Kumar, praveen@gcwtvm.ac.in

ABSTRACT: Glutamine amidotransferase (gatD) catalyze the amidation of the α-carboxyl group of the D-isoglutamate residue in Lipid II resulting in the formation of D-isoglutamine. Mutants deficient in Lipid II amidation show a reduced cross-linking of peptidoglycan and are highly susceptible to antibiotics. Thus, interfering with amidation reaction in gram-positive bacteria may represent a useful strategy to combat the pathogens. In the present investigation, gatD from *Clostridium botulinum* was subjected to homology modelling, phylogenetic analysis and molecular docking. As the crystal structure for gatD was unavailable, the strategy of homology modelling was utilized to generate its tertiary structure. The generated model was refined, energy minimized and validated to ensure the better quality. The phylogenetic analysis revealed the presence of three distinct clusters and highlighted the divergence in gatD polypeptide sequence distributed throughout the gram-positive bacterial species. The ligand binding pockets in gatD and the associated residues were identified using PrankWeb. The results from molecular docking study revealed that Compound 1 (Pubchem CID: 260474), Triciribine, Iodotubercidin, Azasangivamycin, Sangivamycin, Toyocamycin, Tecadenoson, Compound 2 (Pubchem CID: 324510) bind effectively to the ligand binding pocket of gatD with a binding energy of -8.6, -8.3,-8.1, -8.1, -8.0, -7.8, -7.7, -7.1 respectively. As majority of these compounds are also known as anti-cancer, antiviral agents, they are worth of further experimental investigations in terms of inhibition of cell wall synthesis, amidation and anti-microbial properties. Computer-aided drug design is useful for the identification of novel drug targets and to design new drugs. The experimental studies have to be carried to evaluate the amidation interfering properties of the predicted compounds. © 2020 iGlobal Research and Publishing Foundation. All rights reserved.

Cite this article as: Kumar, P.; Mohanan, A.G.; Anil, K.A.K. Homology modelling, phylogenetic analysis and molecular docking of glutamine aminotransferase, gatD from *Clostridium botulinum*. Indo Global J. Pharm. Sci., 2020; 10(4): 46-57. **DOI**: http://doi.org/10.35652/IGJPS.2020.10408 .

INTRODUCTION

The bacterial cell wall mainly consists of a peptidoglycan polymer located external to the cytosolic membrane. The peptidoglycan units consist of the disaccharide *N*-acetylglucosamine and *N*-acetylmuramic acid to which a pentapeptide is attached. The lipid II is a carrier of complete disaccharide-peptide monomer unit. Lipid II is transferred from the cytoplasmic membrane to externally located sites where polymerization of the disaccharide-peptide monomer takes place [1]. The peptide moiety in the lipid II undergoes secondary modifications prior to the polymerization reactions such as amidation, the addition of extra amino acids, and

esterification, etc. Recently, the crystal structure of an enzyme, GatD/MurT complex from *S. aureus* was solved at high resolution [2]. Amidation of the α-carboxyl group of the D-isoglutamate residue in Lipid II results in the formation of D-isoglutamine [3]. This reaction is catalyzed by GatD/MurT complex [4]. This complex comprises of two proteins, GatD and MurT, which assemble into a binary complex. GatD is homologous to the catalytic domains of glutamine amidotransferases, while MurT is identical to the sequence to the substrate-binding domains of Mur ligases. The amidation of α-D-isoglutamic acid of cell wall precursor stem peptides is

catalyzed by GatD/MurT complex in an ATP-dependent reaction [2]. Mutants deficient in Lipid II amidation show a reduced cross-linking of peptidoglycan and are highly susceptible to antibiotics. Thus, interfering with amidation reaction in gram-positive bacteria may represent a useful strategy to combat the pathogens.

Clostridium botulinum is a Gram-positive, rod-shaped bacterium, which produces a neurotoxin, botulinum. Four different groups are recognized within *C. botulinum* in which Groups I and II are primarily responsible for human botulism. A dose of 30–100 ng (3000 MLD_{50}) (mouse minimum lethal doses) of neurotoxin is sufficient to cause human botulism [5]. There are reports confirming the isolation of strains of *C. botulinum* resistance to Penicillin and Metronidazole [6]. Antibiotics could be useful to eliminate *C. botulinum* from the intestine, but this might aggravate botulinum symptoms [7].

Glutamine amidotransferase (gatD) from *C. botulinum is not well characterized and the crystal structure of gatD has not yet been elucidated.* Computer-aided drug design is useful for the identification of novel drug targets and to design new drugs [8].In this paper, we have explored the possibility of using gatD from *C. botulinum* as a drug target. Further, an attempt was made to study the evolutionary relationship among gatD from gram-positive bacterial species.

MATERIALS AND METHODS

Phylogenetic Tree construction
The gatD protein sequences of different gram-positive bacteria were retrieved from Uniprot and the sequences were downloaded in 'fasta' format. The phylogenetic analysis of gatD sequences were carried out using the Molecular Evolutionary Genetic Analysis program version 7.0 [9]. ClustalW algorithm was used for multiple sequence alignment. A neighbour-joining algorithm with 1,000 bootstraps was used in order to infer the evolutionary history. Total sequences involved in the phylogenetic analysis amounted to 47. All positions containing gaps and missing data were eliminated. There were 205 positions in the final dataset.

Homology modelling and validation
The sequence gatD protein of *C.botulinum* was retrieved from Uniprot KB (https://www.uniprot.org/). The sequence in 'fasta' format was submitted to swiss-model workspace to generate a 3-D homology-based model of the protein (model-1) (https://swissmodel.expasy.org/). The model generated in the swiss-model workspace was submitted to 3-D refine

protein structure refinement so as to obtain a refined model (model-2). The model generated in Swiss-model workspace was further subjected to energy minimization in UCSF-Chimera (version-1.13.1) (model-3). MolProbity score, stereochemical property (Ramachandran Plot) and global QMEAN score of all three models was assessed by Ramachandran plot analysis in the swiss structure assessment web server (https://swissmodel.expasy.org/assess). Assessment of protein models with three-dimensional profiles was carried out in VERIFY 3D (https://servicesn.mbi.ucla.edu/Verify3D/) andoverall quality factor for non-bonded atomic interactions was assessed by ERRAT score (https://servicesn.mbi.ucla.edu/ERRAT/)

Molecular Docking
The gatD model obtained by homology modelling and energy minimization (model-2) was submitted to PrankWeb (http://prankweb.cz/)for ligand binding site prediction and conservation Exploration. The model-2 was submitted to SPOT-ligand, an online server for virtual screening [10]. Molecular docking was done by using AutodockVina (version-1.5.6) with chimera (version-1.13.1) used as an interface. The energy minimization was performed both for ligand and receptor and mol2 files were generated. The centre grid coordinates in AutodockVina were identified based on the measurement of the pocket-1(in PrankWeb). The coordinates for grids in AutodockVina were -49×39×37 while size grids used for x, y, z were 20×20×20, respectively. The number of binding modes was fixed at 5. The rest of the parameters were kept in default. Discovery Studio 4.1 visualizer (http: // accelrys.com/products /discovery-studio/) was used for the visualization of docking results of top 8 ligands with gatD.

RESULTS AND DISCUSSION
Phylogenetic Analysis of gatD
The phylogenetic analysis of deduced polypeptide sequences of gatD from gram-positive bacteria revealed the presence of two major and one minor cluster (**Figure 1**). It was found that clusters 1 and 3 were polyphyletic in origin with four and three clades respectively. The cluster I comprised of gatD from *Streptooccus, Enterococcus* and related bacterial species. The gatD from genus *Clostridium and Hathewaya* formed a unique cluster (Cluster II) and is unrelated to cluster III. The gatD from *Staphylococcus, Streptomyces* and related species are included in Cluster III. It was interesting to note that the gatD from *C.botulinum* is evolutionary related to cluster I. All the sequences within a cluster indicated orthologs from different species of gram-positive bacteria. The ancestral gatD sequence has undergone a series of duplication and diversification event in each cluster. Overall, the phylogenetic

tree constructed by the neighbour-joining method indicated considerable divergence in gatD polypeptide sequence

distributed throughout the bacterial species.

Figure 1. Phylogenetic relationships among gatDprotein sequences from gram-positive bacterial species constructed by neighbour-joining algorithm.Theuniport ids are given inparenthesis. The bootstrap values are shown in nodes and are percentages of 1000 replications. The blue coloured upright triangle represents the gatDprotein sequence from *C. botulinum*.
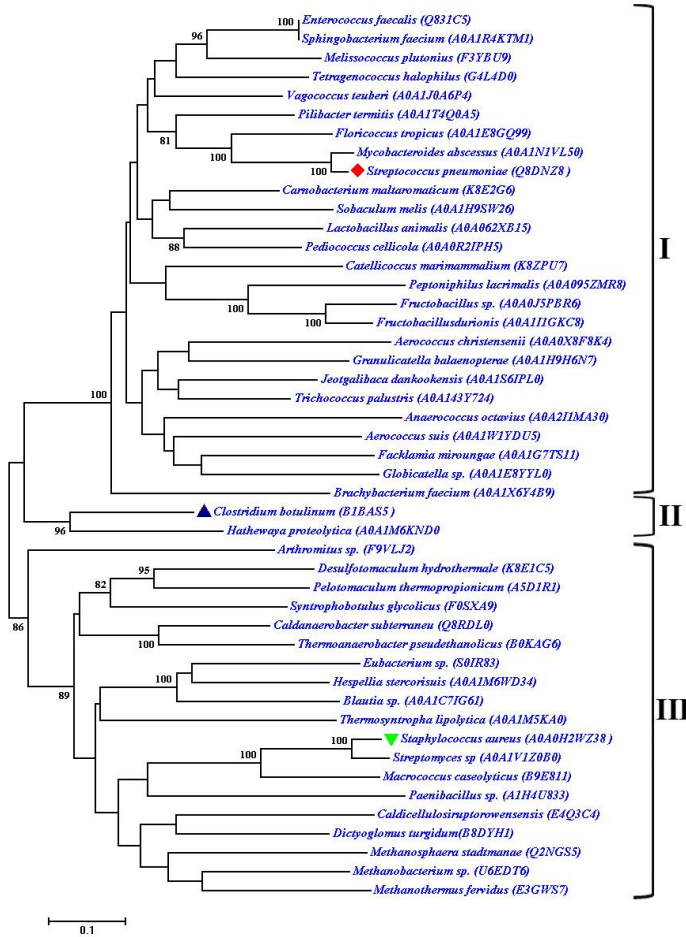
Figure 2. Pairwise alignment of gatD from *S. pneumoniae* and *C. botulinum*
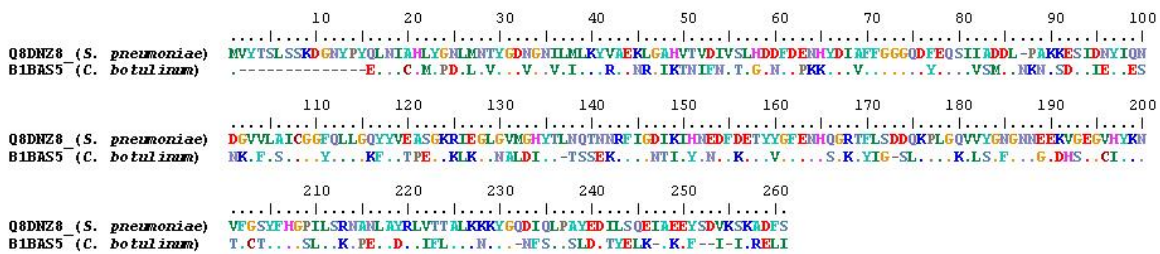
Table 1: Validation of homology- based models of gatD from *C. botulinum*

Models	MolProbity Score	% of Ramachandran favoured residues	QMEAN Z-scores	Verify 3D score	ERRAT score
Model-1	1.73	92.7	-0.51	82.96	97.3
Model-2	1.43	93.45	0.77	84.75	99.5
Model-3	2.01	95.02	-0.25	83.41	88.6

Table 2: Prediction of ligand binding pocket in gatD of *C. botulinum* by using PrankWeb

Name	Rank	Conservation Score	Coordinate Center-x	Coordinate Center-y	Coordinate Center-z	Amino acid residues associated with pockets
Pocket 1	1	30.3525	-46.9701	38.9523	36.7012	Tyr103, Val104, Pro106, Thr123, Arg127, Asn148, Val14, His149, Ser150, Gly151, Tyr15, Tyr188, His190, Gly58, Gly59, Gln60, Asp61, Gly64, Cys93, Gly94, Gln97
Pocket 2	2	1.4414	-44.5581	55.7616	33.3535	Thr153, Ile155, Asn171, Glu173, His175, Ser176
Pocket 3	3	0.9354	-57.0919	60.2349	44.3219	Asp138, Phe140, Ile180, Tyr181, Lys182, Asn183

Table 3: Table showing list of compounds, molecular weight, autodock vina binding energy, number of H-bonds formed and residues in the pocket involved in H-bonding.

| Ligands	Molecular weight (g/mol)	Autodockvina binding energy (kcal/mol)	No. of H-bond formed	Residues in pocket involved in H-bonding
Compound 1 (Pubchem CID: 260474)	325.28	-8.6	6	Gly59, Asp61, Gln64, Gly94, Arg127, Ser150
Triciribine	320.3	-8.3	3	Asp61, Ser150, His190
Iodotubercidin	392.15	-8.1	5	Gly59, Asp61, Gln64, Gln97, Asn128
Azasangivamycin	310.27	-8.1	5	Gly59, Gln64, Gln97, Asn148, His190
Sangivamycin	309.28	-8	3	Gln64, Gln97, Asn148
Toyocamycin	291.26	-7.8		
Tecadenoson	337.33	-7.7	3	Gly59, Gln97, His190
Compound 2 (Pubchem CID: 324510)	295.29	-7.1	3	Gly59, Gln97, His190

Figure 3. Ramachandran plot of gatD from *C. botunilum*. A:-Homology models generated by Swiss-model (model-1), B:- model obtained by energy minimization in Chimera (model-2) and C:- model refined by 3-D refine (model-3).
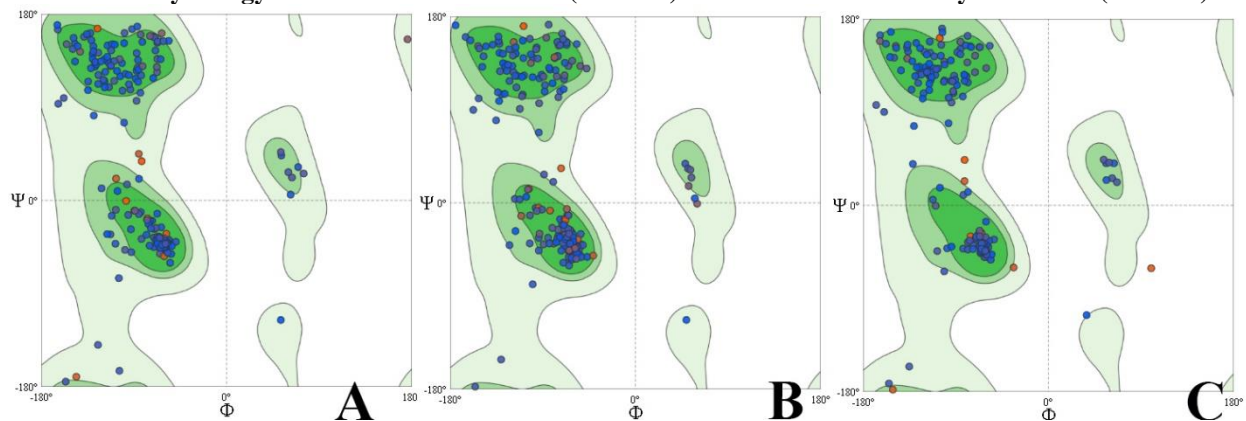
Table 4. Chemical structure and IUPAC names of the compounds used for molecular docking

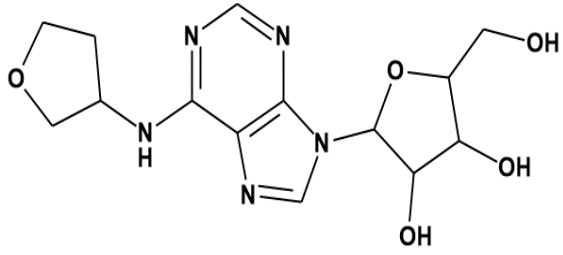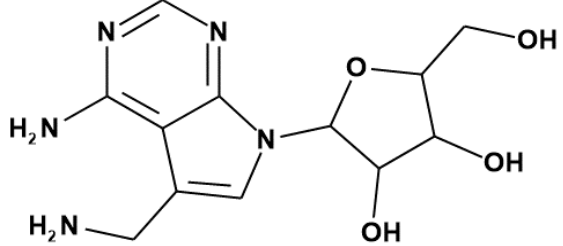| Compound Name and Pubchem CID	IUPAC name	Structure
Compound 1 (260474)	N-[9-[3,4-dihydroxy-5-(hydroxymethyl)oxolan-2-yl]-8-oxo-7H-purin-6-yl]acetamide	
Triciribine (65399)	(2R,3R,4S,5R)-2-(5-amino-7-methyl-2,6,7,9,11-pentazatricyclo[6.3.1.0^{4,12}]dodeca-1(12),3,5,8,10-pentaen-2-yl)-5-(hydroxymethyl)oxolane-3,4-diol	
Iodotubercidin (46875276)	(3R,4S,5R)-2-(4-amino-5-iodopyrrolo[2,3-d]pyrimidin-7-yl)-5-(hydroxymethyl)oxolane-3,4-diol	
Azasangivamycin (98801)	4-amino-1-[(2R,3R,4S,5R)-3,4-dihydroxy-5-(hydroxymethyl)oxolan-2-yl]pyrazolo[3,4-d]pyrimidine-3-carboxamide	
Sangivamycin (14978)	4-amino-7-[(2R,3R,4S,5R)-3,4-dihydroxy-5-(hydroxymethyl)oxolan-2-yl]pyrrolo[2,3-d]pyrimidine-5-carboxamide	
Toyocamycin (11824)	4-amino-7-[(2R,3R,4S,5R)-3,4-dihydroxy-5-(hydroxymethyl)oxolan-2-yl]pyrrolo[2,3-d]pyrimidine-5-carbonitrile	

Tecadenoson (158795)	(2*R*,3*S*,4*R*,5*R*)-2-(hydroxymethyl)-5-[6-[[(3*R*)-oxolan-3-yl]amino]purin-9-yl]oxolane-3,4-diol	
Compound 2 (324510)	**2-[4-amino-5-(aminomethyl)pyrrolo[2,3-d]pyrimidin-7-yl]-5-(hydroxymethyl)oxolane-3,4-diol**	

Figure 4. Structure comparison of gatD from *C. botunilum*: Homology models generated by Swiss-model(blue), model refined by 3-D refine (red) and model obtained by energy minimization in Chimera (yellow).
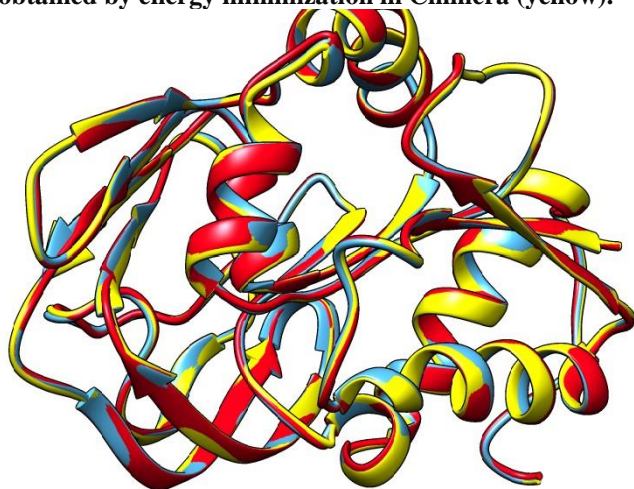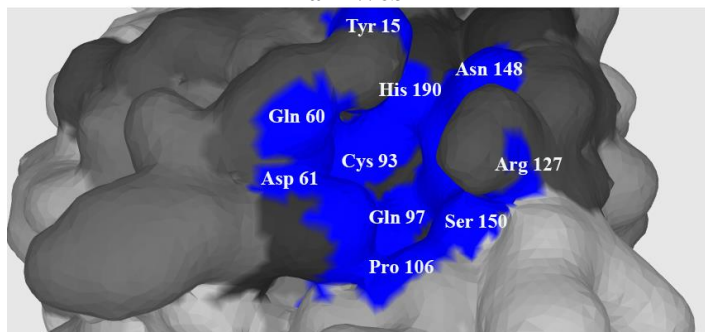

Figure 5. 3D image of pocket-1 of gatD as predicted by PrankWeb

Protein structure prediction and validation

The 240 amino acids residue long gatD protein of *C. botulinum* was subjected to Swiss-model

(https://swissmodel.expasy.org/) for comparative protein modelling. Comparative homology modelling depends on a sequence alignment between target sequence and the template sequence whose 3D structure has been determined by the experimental method. The results obtained from Swiss-modelling server indicated that the target sequence is 52.7% identical to GatD from *Streptococcus pneumonia* (6FQB). GMQE (Global Model Quality Estimation) score is expressed as a number between 0 and 1 and reflects the expected accuracy of a model built with that alignment and template and the coverage of the target. A GMQE score of 0.77 was obtained which indicated higher reliability. The QMEAN Z-score provides an estimate of the "degree of nativeness" of the structural features observed in the model on a global scale. QMEAN Z-scores nearing zero indicate good agreement between the model structure and experimental structures of similar size. In the present investigation, we found that the QMEAN Z-score of gatD is -0.51 which is within the acceptable range, indicating a good quality model. The pairwise sequence alignment of gatD protein of *C. botulinum* (B1BAS5) and gatD protein *Streptococcus pneumonia* (Q8DNZ8) is shown in **Figure 2**. The homology model of gatD from *C. botulinum* was further subjected to energy minimization by using Chimera (version-1.13.1) and structural refinement by using 3-D refine (online server for protein structural refinement) [11]. The results of structural refinement through 3-D refine and energy minimization in Chimera are shown in **Table 1**. The validation for the generated models was done on the basis of Ramachandran plot, MolProbity Score, QMEAN Z-score, Errat Score and Verify 3D score. The *MolProbity* is a structure-validation web service that provides evaluation of protein and nucleic acid model quality at both the global and local levels [12]. Lower *MolProbity* scores are supposed to represent better quality models. We found that *MolProbity scores of all models are in an acceptable range*. The overall stereochemical quality of the

modelled 3D structure of proteins was evaluated by using the Ramachandran plot which is based on psi (Cα-C bond) and phi (N-Cα bond) angles of the protein and provides information about the number of amino acid residues present in allowed and disallowed regions. We found that the model generated by energy minimization and refinement by 3D refine web server consisted of 93.45 and 95% amino acid residues respectively in the favoured region, whereas the initial model shows 92.7 % of residues in the most favoured region (**Figure 3, Table 1**). Verify 3 D determines the compatibility of an atomic model with its own amino acid sequence by assigning a structural class based on its location and environment and comparing the

results to good structures. All the models generated in this study qualified the criterion used by Verify3D with more than 80% of the residues having averaged 3D-1D score >= 0.2. The ERRAT scores of the models ranged from 88.8 to 97.3. Interestingly, the ERRAT score of the refined model was less when compared to the initial model and energy minimized one (**Table 1**). Overall the results indicated that models generated by energy minimization and refinement are more sophisticated and more conformationally better when compared to the initial model. The Figure4 shows the comparison of initial, refined model and energy minimized model in UCSF chimera.

Figure6. gatD ligand binding pocket – compound 1 interaction. A) 3D representation of interaction between compound 1 and residues in gatD ligand binding pocket. B) 2D interaction diagram of compound 1 with residues in gatD ligand binding pocket.
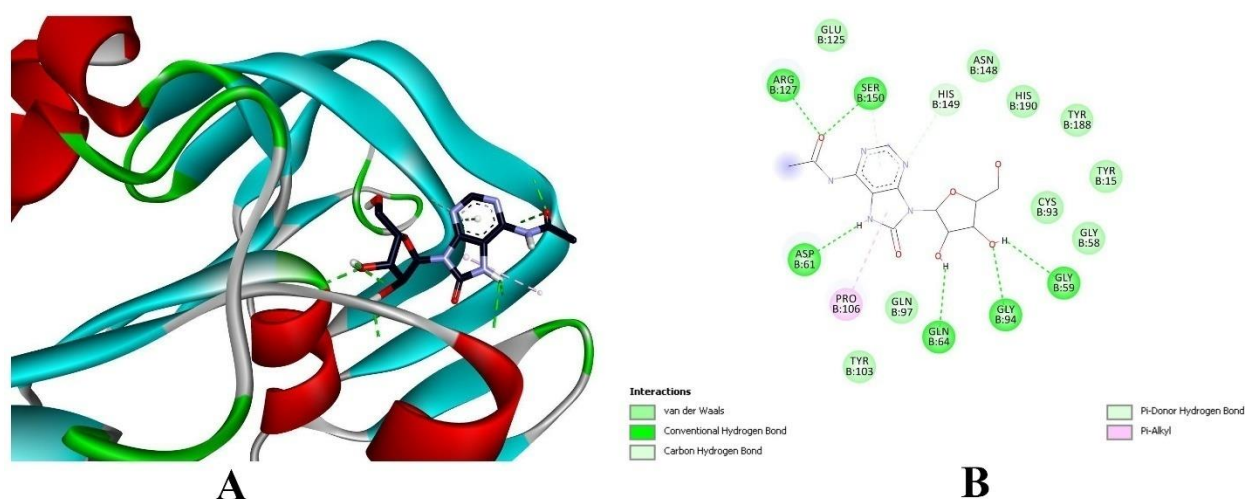

Figure7. gatD ligand binding pocket–Triciribine interaction. A) 3D representation of interaction between Triciribine and residues in gatD ligand binding pocket. B) 2D interaction diagram of Triciribine with residues in gatD ligand binding pocket.
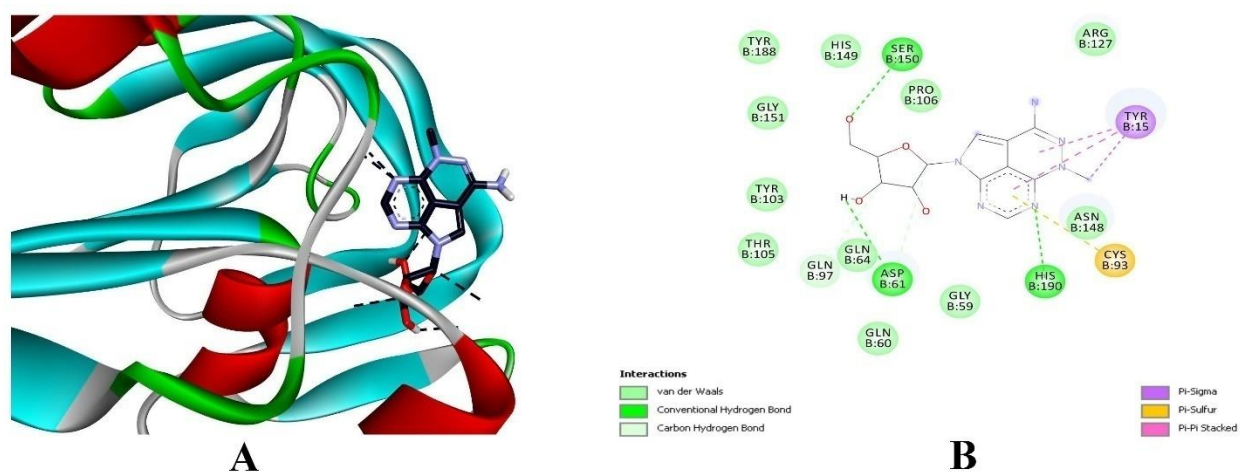
Figure8. gatD ligand binding pocket–Iodotubercidin interaction. A) 3D representation of interaction between Iodotubercidin and residues in gatD ligand binding pocket. B) 2D interaction diagram of Iodotubercidin with residues in gatD ligand binding pocket.
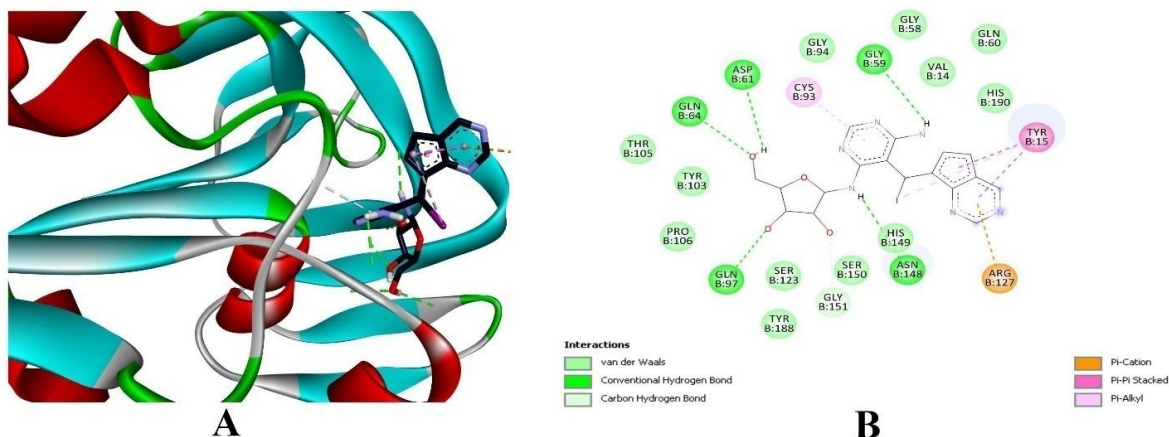

Figure9. gatD ligand binding pocket–Azasangivamycin interaction. A) 3D representation of interaction between Azasangivamycin and residues in gatD ligand binding pocket. B) 2D interaction diagram of Azasangivamycin with residues in gatD ligand binding pocket.
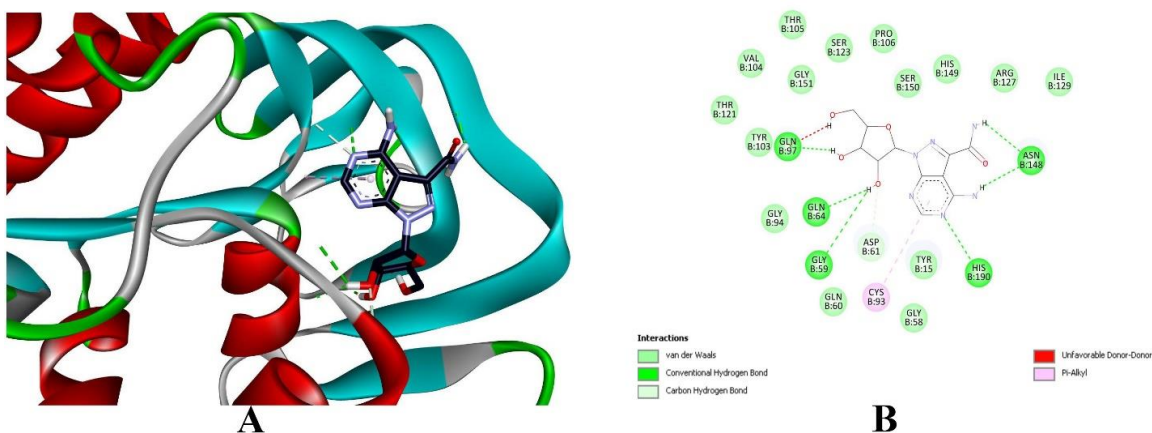

Figure 10. gatD ligand binding pocket–sangivamycin interaction. A) 3D representation of interaction between sangivamycin and residues in gatD ligand binding pocket. B) 2D interaction diagram of sangivamycin with residues in gatD ligand binding pocket
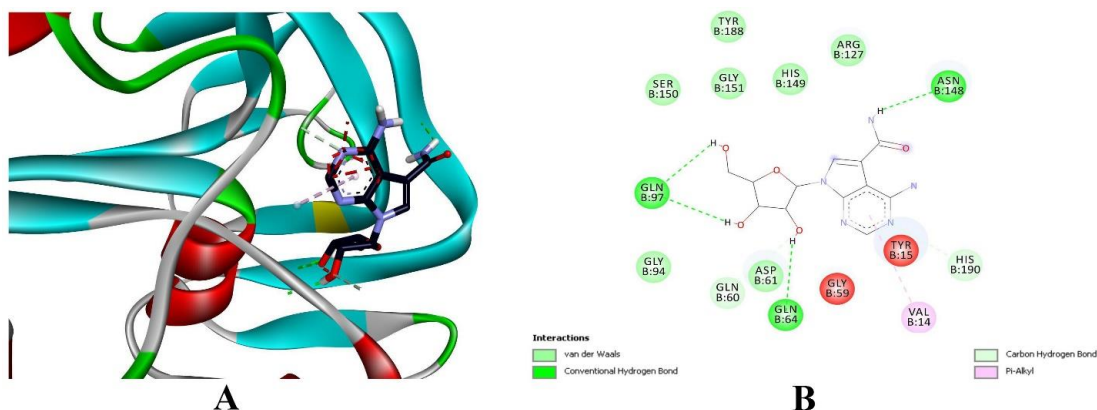
Figure 11.gatD ligand binding pocket–Toyocamycin interaction. A) 3D representation of interaction between Toyocamycin and residues in gatD ligand binding pocket. B) 2D interaction diagram of Toyocamycin with residues in gatD ligand binding pocket.
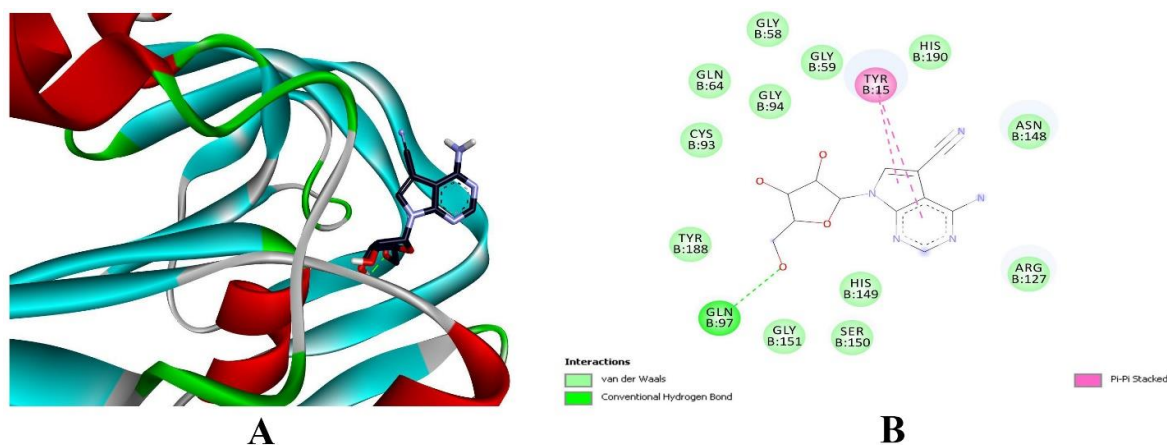

Figure 12.gatD ligand binding pocket–Tecadenoson interaction. A) 3D representation of interaction between Tecadenoson and residues in gatD ligand binding pocket. B) 2D interaction diagram of Tecadenoson with residues in gatD ligand binding pocket
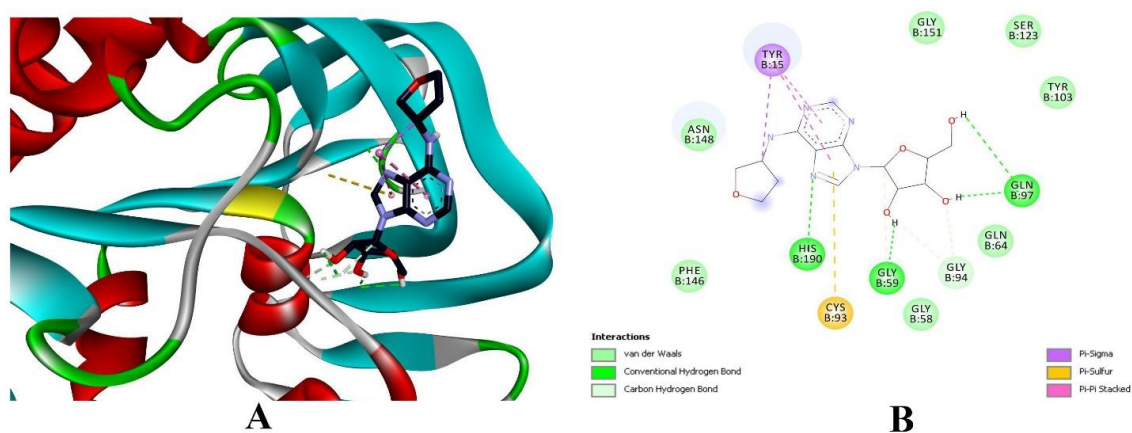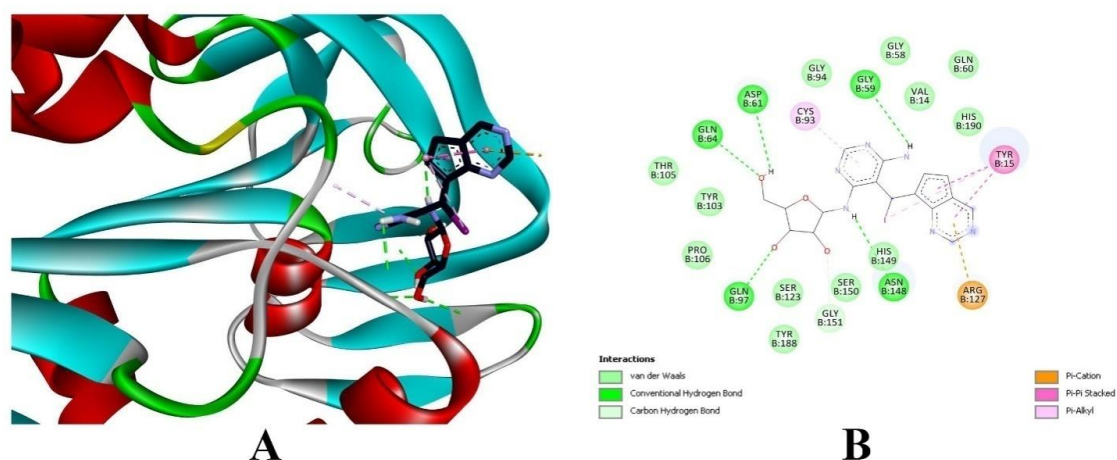

.

Figure 13.gatD ligand binding pocket–Compound 2 interaction. A) 3D representation of interaction between Compound 2 and residues in gatD ligand binding pocket. B) 2D interaction diagram of Compound 2 with residues in gatD ligand binding pocket.

Ligand binding site prediction

The ligand binding site of gatD was searched by using PrankWeb (http://prankweb.cz/). Three ligand binding pockets were predicted out of these the pocket-1 (with highest conservation score of 30.3) was selected (**Table 2, Figure 5**). The pocket-1 is composed of a larger number of residues than any of the other pockets (21 amino acids). The 3D coordinate of pocket 1 is centred around x (-46.9701), y (38.9523) and z (36.7012) (**Table 2**).

Molecular Docking of gatD with small molecules

From the list of 1000 ligands obtained in SPOT-Ligand virtual screening, 30 compounds were subjected to molecular docking by using autodockvina. We further identified Triciribine phosphate (ZINC05385245) from the aforementioned list and subsequently docked Triciribine and related compounds (from Pubchem) with gatD. The list of compounds, molecular weight, and autodockvina binding energy are shown in Table 3. The autodock binding energy ranged from -7.1 to -8.6. The molecular weight of the ligands ranged from 295 to 392. In autodockvina, the best binding energy was exhibited by compound 1 (-8.6 kcal/mol) followed by Triciribine (-8.3 kcal/mol). The ligand poses with the highest binding energy and RMSD=0 were selected as the best pose. Discovery Studio 4.1 visualizer was employed to study the nature and types of interaction between residues of ligand binding pocket in gatD and compounds (**Figure 6-13**). We found that various non-covalent interactions viz. Hydrogen bond, Van der Waals interactions, Pi-alkyl interactions, alkyl interactions, Pi-cation interactions and Pi-Pi T shaped interactions between ligands and amino acid residues in the ligand binding pocket. The *hydrogen bonds* are a *significant* factor that contributes to the stability *of protein-ligand* binding *interactions in molecular docking [13].*The most frequent residues in the ligand binding pocket of gatD domain involved in hydrogen bond formation with ligands were Gly59, Gln64, His190 and Gln97. The maximum number of hydrogen bonds (6 numbers) were formed by compound 1with the ligand binding pocket of gatD which correlates with high autodock vina binding energy (Table 3).Triciribine is a nucleoside analogue with a pentaazaacenaphthylene ring system linked with ribofuranosyl moiety by a glycosidic linkage (**Table 4**).Triciribine phosphate, a potent anti-cancer drug [14]and inhibitor of AKT (Protein Kinase B), is currently undergoing clinical trial against breast cancer (A study of PTX-200 (Triciribine) plus Cytarabine in refractory or relapsed Acute Leukemia. https://clinicaltrials.gov/ct2/show/NCT02930109, accessed on 3/1/2020). The compound 1 is related to

triciribine but contain a ribofuranosyl moiety linked to a dihydropurine instead of pentaazaacenaphthylene ring (**Table 4**). The biological activity and target of the compound 1 are not yet identified. Iodotubericidin is an Iodopyrrolopyrimidine linked with ribofuranosyl moiety (**Table 4**). It is anti-tumour drug and strong p53 activator and used as an inhibitor for various kinases including adenosine kinase [15]. Sangivamycin, toyocomycin and compound 2 have pyrrolopyrimidine ring linked with ribofuranosyl moiety (**Table 4**).Sangivamycin is an anti-tumour agent and a potent inhibitor of protein kinase C [16] (**Table 4**). Toyocamycin is an N-glycosylpyrrolopyrimidine in which the hydrogen at position 5 of the pyrrolopyrimidine moiety has been replaced by a cyano group (**Table 4**). Toyocamycin has antibiotic, antiviral as well as cytotoxic properties, and is known to inhibit the maturation of 40 S subunit of ribosome [17]. It acts as an antimetabolite, an antifungal agent, an antineoplastic agent, a bacterial metabolite and an apoptosis inducer. The biological activity and target for compound 2 is not yet identified. Tecadenoson is a selective A1 receptor agonist, which has been studied for their use against arrhythmia and atrial fibrillation [18]. Azasangivamycin is an analog of Sangivamycin in which the pyrrolopyrimidine ring is replaced by pyrazolopyrimidine. Azasangivamycin inhibits anti-viral properties and is active against Human cytomegalovirus and Herpes Simplex type I virus [19]. To conclude, except compound 1 and 2 all other compounds are reported as biologically active. gatD is an enzyme involved in amidation of α-D-isoglutamicacid of cell wall precursor stem peptides in *S. aureus.* It has been demonstrated that *S. aureus* mutants defective in amidation are less viable and show increased susceptibility to antibiotics [2]. Therefore, inhibition of amidation reaction offers a novel strategy to combat *S. aureus* and other gram-positive bacterial pathogens such as *C. botulinum.* None of the compounds identified in this study were previously known as inhibitors of the gatD enzyme or amidation reaction. Therefore, we predict that all compounds identified via molecular docking are potential inhibitors of the gatD enzyme and amidation reaction. We further hypothesize that the compounds identified in this study can be developed as anti-amidation drugs in the near future. To the best of our knowledge, this is not only the first report of exploiting gatD as drug target but also prospective identification of anti-amidation drugs. The compounds identified in this study can be used against infections caused by *C. botulinum* in the future. Further experimental studies are needed to support our hypothesis.

CONCLUSION

The present study was undertaken for molecular and *in silico* characterization of gatD from *C. botulinum*. As the crystal structure for gatD was unavailable in the PDB databank, the strategy of homology modelling was utilized to generate its 3D structure. The generated model was refined and energy minimized and further validated to ensure better quality. The phylogenetic analysis revealed the presence of three distinct clusters and highlighted series of duplication and diversification events in each cluster. The ligand binding pockets in gatD and the associated residues were identified using PrankWeb. Further, this study is first of its kind to predict the molecular mechanism(s) underlying the docking of series of anti-amidation agent to the target enzyme, gatD, indicating the tremendous potential of these agents in hindering the growth of *C. botulinum* and other related species. As the majority of these compounds are also known as anti-cancer and antiviral agents, they are worth of further experimental investigations in terms of inhibition of cell wall synthesis, amidation and anti-microbial properties. The findings of this study are expected to have an impact on the current emergence of research focus on the novel species-specific antimicrobial agents by investigating the unexplored aspects of the molecular nature of its interaction with target enzyme, gatD.

ACKNOWLEDGEMENT

CONFLICTS OF INTEREST

None.

DATA AVAILABILITY

The data used to support the findings of this study are included within the article.

FUNDING SOURCE

REFERENCES

[1] Van Heijenoort, J. Lipid Intermediates in the Biosynthesis of Bacterial Peptidoglycan.Microbiol. Mol. Biol. Rev., 2007; 71(4):620-635.

[2] Nöldeke, E.R. et al. Structural basis of cell wall peptidoglycan amidation by the GatD/MurT complex of *Staphylococcus aureus*. Scientific Reports., 2018; 8(1):1-15.

[3] Gotz, F., Bannerman, T.,Schleifer, K.H. The Genera *Staphylococcus* and *Macrococcus*.Prokaryotes. In: A Handbook on the Biology of Bacteria, 3[rd]ed; Springer, 2006; 4: 45-75

[4] Münch, D., Roemer, T., Lee, S.H., Engeser, M., Sahl,HG., Schneider, T. Identification and in vitro analysis of the GatD/MurT enzyme-complex catalyzing lipid II amidation in *Staphylococcus aureus*. PLoS Pathogens., 2012; 8(1).

[5] Carter, A.T., Peck, M.W. Genomes, neurotoxins and biology of *Clostridium botulinum* Group I and Group II. Research in Microbiology., 2015; 166(4):303–17.

[6] Mazuet, C., Legeay, C., Sautereau, J., Ma, L., Bouchier, C., Bouvet, P.,Popoff, M.R. Diversity of group I and II *Clostridium botulinum* strains from France including recently identified subtypes: Genome Biology and Evolution., 2016; 8:1643-60.

[7] Fenicia, L., Anniballi, F. Infant botulism. Ann.Ist. Super.Sanita., 2009;45(2):134-146.

[8] Katsila, T., Spyroulias, G.A., Patrinos, G.P.,Matsoukas, M.T. Computational approaches in target identification and drug discovery. Computational and Structural Biotechnology Journal., 2016; 14:177–184.

[9] Kumar, S., Stecher, G., Tamura, K. MEGA7: Molecular Evolutionary Genetics Analysis Version 7.0 for Bigger Datasets., Molecular biology and evolution., 2016; 33:1870-74.

[10] Litfin, T., Zhou, Y., Yang Y. SPOT-ligand 2.improving structure-based virtual screening by binding-homology search on an expanded structural template library. Bioinformatics., 2017; 33:1238-1240.

[11] Bhattacharya, D., Nowotny,.J, Cao, R., Cheng, J. 3Drefine: an interactive web server for efficient protein structure refinement. Nucleic acids research., 2016; 44:406-9.

[12] Chen, V.B. et al. MolProbity: All-atom structure validation for macromolecular crystallography.ActaCrystallographica., 2010; 66(1) 12–21.

[13] Patil, R., Das, S., Stanley, A., Yadav, L., Sudhakar, A.,Varma, A.K. Optimized hydrophobic interactions and hydrogen bonding at the target-ligand interface leads the pathways of drug-designing. Plos One., 2010; 5:1

[14] Garrett, C.R. et al. Phase I pharmacokinetic and pharmacodynamic study of Triciribine phosphate monohydrate, a small-molecule inhibitor of AKT phosphorylation, in adult subjects with solid tumors containing activated AKT. Investigational New Drugs., 2011; 29:1381-9.

[15] Zhang, X. et al. Identification of 5-Iodotubercidin as a Genotoxic Drug with Anti-Cancer Potential. PLoS One., 2013; 8(5)

[16] Loomis, C.R., Bell, R.M. Sangivamycin, a nucleoside analogue, is a potent inhibitor of protein kinase C. Journal of Biological Chemistry., 1988; 263:1682–1692.

[17] Kiburu, I.N., LaRonde-LeBlanc, N. Interaction of Rio1 Kinase with Toyocamycin Reveals a Conformational Switch That Controls Oligomeric State and Catalytic Activity. PLoS One., 2012; 7(5)

[18] Rabuffetti, M., Bavaro, T., Semproli.R., Cattaneo, G., Massone, M., Morelli, C.F.Synthesis of Ribavirin, Tecadenoson, and Cladribine by Enzymatic Transglycosylation. Catalysts., 2019; 9(4):355.

[19]Migawa, M.T., Drach, J.C., Townsend, L.B.Design, Synthesis and Antiviral Activity of Novel 4,5-Disubstituted 7-(β- d Ribofuranosyl)pyrrolo[2,3- d][1,2,3]triazines and the Novel 3-Amino-5-methyl-1-(β- d -ribofuranosyl)- and 3-Amino-5-methyl-1-

(2-deoxy-β-   d   -ribofuranosyl)-1,5-dihydro-1,4,5,6,7,8-hexaazaacenaphthylene as Analogues of Triciribine Journal of Medicinal Chemistry., 2005; 48:3840-3851.